Smart Structures and Systems, *Vol. 23, No. 1 (2019) 31-44*
DOI: https://doi.org/10.12989/sss.2019.23.1.031

Influence of surface irregularity on dynamic response induced due to a moving load on functionally graded piezoelectric material substrate

Abhishek K. Singh*, Anil Negi and Siddhartha Koley

Department of Applied Mathematics, Indian Institute of Technology (Indian School of Mines), Dhanbad-826004, Jharkhand, India

(Received April 13, 2018, Revised November 28, 2018, Accepted November 30, 2018)

Abstract. The present study investigate the compressive stress, shear stress, tensile stress, vertical electrical displacement and horizontal electrical displacement induced due to a load moving with uniform velocity on the free rough surface of an irregular transversely isotropic functionally graded piezoelectric material (FGPM) substrate. The closed form expressions of said induced stresses and electrical displacements for both electrically open condition and electrically short condition have been deduced. The influence of various affecting parameters viz. maximum depth of irregularity, irregularity factor, parameter of functionally gradedness, frictional coefficient of the rough upper surface, piezoelectricity/dielectricity on said induced stresses and electrical displacements have been examined through numerical computation and graphical illustration for both electrically open and short conditions. The comparative analysis on the influence of electrically open and short conditions as well as presence and absence of piezoelectricity on the induced stresses and induced electrical displacements due to a moving load serve as the salient features of the present study. Moreover, some important peculiarities have also been traced out by means of graphs.

Keywords: functionally graded piezoelectric material; moving load; stress; electrical displacement; irregularity

1. Introduction

The investigation of stresses induced due to a moving load on an elastic medium is a topic of great concern due to its applications towards stability of the medium. Because if the shear stress induced due to a moving load on the medium is more than shear strength of the medium, the failure of structure occurs. Therefore, due to having possible applications in measuring the stability of the structure, the problem of dynamic response of medium subjected to a moving load has been received consideration attention from past few decades in the field of geophysics, seismology, civil engineering, etc. (Hearle and Johnson 1985, De Barros and Luco 1994, Fryba 1999, Sheng *et al.* 1999). In recent years, due to increase in high speed train networks, it becomes imperative to examine the stability of medium under the effect of dynamic load. Various type of structures used in transportation viz. bridges, guide waves, cableways, rails, roadways and runways are subjected to moving loads. Irrespective of other dynamic load, the impact of moving load vary with respect to the position, therefore, the problem of a moving load is an emerging topic in structural dynamics to examine the instability occur in structure (Olsson 1991). An elastic material can be considered to be transversely isotropic if the elastic properties of the material vary vertically but not horizontally in the simplest horizontal or layered case. Several theoretical and experimental studies show that there always exist irregularity of different shape and size in elastic materials. The irregularity occurs in the medium due to various physical phenomena viz. weathering, erosion or other external force. Therefore, due to inclusion of irregularity in elastic medium, the mathematical model of the problem becomes more realistic. The materials that become electrically polarized under the influence of mechanical stress called piezoelectric materials. The electric polarization in piezoelectric material can be expressed mathematically as the combination of matrices expressing stress and coefficients representing piezoelectricity (Ogawa and Utada 2000). Therefore, piezoelectric materials can be considered as the materials possessing coupling between mechanical and electric fields. The piezoelectric materials also exhibit inverse piezoelectric effect in which such materials experience elastic strain under the application of electric field. Due to this type of reversible nature, piezoelectric crystals are used in numerous applications including embedded sensors and actuators in smart structures, production and detection of sound, sonar, air ultrasonic transducers, electronic frequency generation, filters and delay lines which are widely used in electronic technology, mechanical and medical engineering (Piliposian and Danoyan 2009). The heterogeneity in an elastic medium is caused by variation in rigidity and density. The heterogeneity of the medium can be expressed mathematically as a function of vertical depth (Meissner 2002). The concept of heterogeneity in piezoelectric material is extensively used in in terms of functionally gradedness which can be further used in numerous applications viz. aerospace structures, electronic devices

*Corresponding author, Ph.D.
E-mail: abhi.5700@gmail.com
[a] Ph.D. Student
E-mail: negi.anil3@gmail.com
[b] Ph.D. Student
E-mail: siddharthakoley.ism@gmail.com

 ISSN: 1738-1584 (Print), 1738-1991 (Online)

and many other fields of engineering. In recent years, due to evolution of material technology to manufacture several electronic and electric devices, new type of materials called functionally graded piezoelectric materials (FGPM) have come into existence. These particular type of materials are extensively used to upgrade efficiency and life of SAW devices (Li, Wang and Huang, 2004). Piezoelectric device can produce electric current by means of piezoelectric crystals. Due to having larger power densities and higher feasibility, piezoelectric materials can be used in piezo technology for road construction (Kong *et al.* 2014). In the present scenario, the piezo technology is used to obtain electrical energy as a response of mechanical stress induced due to a moving load on the piezoelectric crystal which may be placed at a shallow depth from the road surface. In general, the electrical energy generates after the slight deformation of piezoelectric crystal under the influence of mechanical stresses induced due to a moving load. Therefore, the study of moving load over a piezoelectric substrate may lead to significant advances in the harvesting of mechanical waste energy by using mechanical vibrations to electricity conversion (Kong *et al*. 2014, Beeby *et al.* 2006). This fact serves as a motivation for the authors to study the problem of a moving load on an irregular transversely isotropic functionally graded piezoelectric material (FGPM) substrate.

The steady state solution of the problem of a normal moving load over an elastic half space was given by Cole and Huth (1958). Sackman (1961) investigated the dynamic response of layered half plane due to a normal moving load. Several authors adopted systematic approach to solve the problem of a moving load (Achenbach 1967, Chonan 1976, Ungar 1976, Olsson 1991). Dieterman and Metrikine (1997) examined the influence of a point harmonic load moving over an elastic layer resting on a rigid foundation. Tondreau *et al.* (2013) discussed about the design of a point load actuator based on flat triangular piezoelectric patches with the use of its geometrical and piezoelectric properties. Mukhopadhyay (1965) examined the stresses induced due to a normal moving load over the surface of a transversely isotropic ice-sheet floating on water. Later on, Mukherjee (1969) studied the problem of moving load on a transversely isotropic elastic solid over a rough free surface. The stresses induced on a rough irregular isotropic half-space due to normal moving load were investigated by Chattopadhyay *et al.* (2011). Chatterjee and Chattopadhyay (2017) discussed the influence of a moving load over the irregular surface of ice-sheet floating over water. Singh *et al.* (2014) discussed the influence of irregularity and heterogeneity on the stresses induced due to a normal moving load on a rough monoclinic half-space. Later on, the effect of irregularity on transversely isotropic piezoelectric medium was discussed by Singh, Kumar, and Chattopadhyay (2015). Several researchers accomplished notable work in context of functional gradient property in piezoelectric materials (Li *et al*. 2004, Qian *et al.* 2007). The coupled electro-elastic effect on functionally graded piezoelectric material plates using trigonometric functions and Lagrange polynomials has been studied by Wu *et al.* (2015).

In view of above facts, it can be seen that numerous studies have been done to investigate the influence of dynamic response due to a moving load on semi-infinite medium under the consideration of different medium properties viz. transversely isotropic, irregularity, heterogeneity, etc. However, to the best of authors knowledge, the stresses induced due to a moving line load on irregular functionally graded piezoelectric material (FGPM) substrate have not been examined till date. In the present analysis, the dynamic response induced due to a load moving with uniform velocity on the rough surface of an irregular transversely isotropic functionally graded piezoelectric material substrate has been examined by obtaining the closed form expressions of induced incremental stresses (compressive, shear and tensile) and electrical displacements (horizontal and vertical) for both electrically open and short boundary conditions. In addition to this, the effects of various affecting parameters viz. maximum depth of irregularity, irregularity factor (corresponding to different cases of irregularity i.e., rectangular irregularity, parabolic irregularity and no irregularity), parameter of functionally gradedness, frictional coefficient due to the roughness of upper surface of the substrate and piezoelectricity/dielectricity on said induced stresses and electrical displacements have been studied numerically as well as demonstrated graphically. The comparative study has been carried out to reveal the effect of electrically open and short conditions and also the effect of presence and absence of piezoelectricity on the induced stresses and induced electrical displacements due to a moving load.

2. Formulation and solution of the problem

Let us consider a line load F moving with a constant velocity V in the positive direction of x-axis in an irregular transversely isotropic functionally graded piezoelectric material (FGPM) substrate. The z-axis is pointing vertically downwards and representing the vertical depth of aforesaid substrate while x-axis represent the direction in which load moves. An irregularity of parabolic shape with span $2a_1$ and maximum depth of irregularity H exist on the upper surface of substrate. The origin is placed at the middle point of span of the surface irregularity as depicted in Fig. 1.

The equation of upper surface of FGPM substrate containing irregularity is

$$z = \varepsilon h(x) \tag{1}$$

where

$$h(x) = \begin{cases} 0, & \text{for} \quad |x| > a_1 \\ \dfrac{2}{a_1}(a_1^2 - x^2), & \text{for} \quad |x| \le a_1 \end{cases}$$

and ε is the small positive number such that $\varepsilon = \dfrac{H}{2a_1} << 1$.

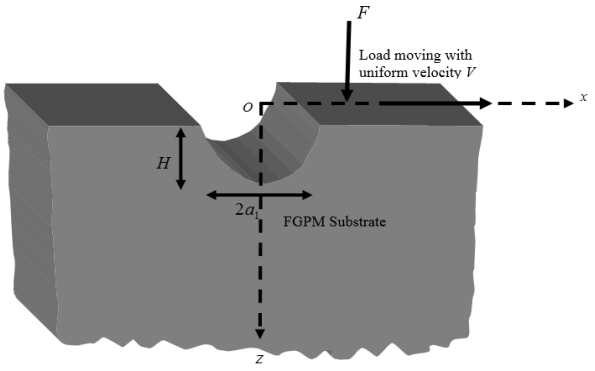

Fig. 1 Geometry of the problem

For plain-strain deformation, it has been considered that

$$u_x = u_x(x,z,t)\ ,u_y = 0,\ u_z = u_z(x,z,t),\ \phi = \phi(x,z,t)\ \text{and}\ \frac{\partial}{\partial y} = 0. \quad (2)$$

where (u_x, u_y, u_z) denote the components of mechanical displacement and ϕ is electrical potential function due to a moving load in considered piezoelectric substrate.

In view of Haojiang (1997); Singh, Kumar, and Chattopadhyay (2015) and Li *et al.* (2004), the stress-strain relations for functionally graded piezoelectric material substrate under plain-strain deformations condition (2) can be written as

$$\left.\begin{aligned}
\tau_{xx} &= e^{\upsilon z}\left(c_{11}^0\frac{\partial u_x}{\partial x} + c_{13}^0\frac{\partial u_z}{\partial z} + e_{31}^0\frac{\partial \phi}{\partial z}\right),\\
\tau_{zz} &= e^{\upsilon z}\left(c_{13}^0\frac{\partial u_x}{\partial x} + c_{33}^0\frac{\partial u_z}{\partial z} + e_{33}^0\frac{\partial \phi}{\partial z}\right),\\
\tau_{zx} &= e^{\upsilon z}\left(c_{44}^0\left(\frac{\partial u_x}{\partial z} + \frac{\partial u_z}{\partial x}\right) + e_{15}^0\frac{\partial \phi}{\partial x}\right),\\
D_x &= e^{\upsilon z}\left(e_{15}^0\left(\frac{\partial u_x}{\partial z} + \frac{\partial u_z}{\partial x}\right) - \varepsilon_{11}^0\frac{\partial \phi}{\partial x}\right),\\
D_z &= e^{\upsilon z}\left(e_{31}^0\frac{\partial u_x}{\partial x} + e_{33}^0\frac{\partial u_z}{\partial z} - \varepsilon_{33}^0\frac{\partial \phi}{\partial z}\right).
\end{aligned}\right\} \quad (3)$$

where c_{ij}^0 represent the values of elastic constants c_{ij} at $z = 0$; e_{ij}^0 signify the values of piezoelectric constants e_{ij} at $z = 0$; ε_{ij}^0 denote the values of dielectric constants ε_{ij} at $z = 0$.

In view of (3), the equations of motion for functionally graded transversely isotropic piezoelectric substrate can be written as

$$\begin{aligned}
&c_{11}^0\frac{\partial^2 u_x}{\partial x^2} + \left(c_{13}^0 + c_{44}^0\right)\frac{\partial^2 u_z}{\partial z \partial x} + (e_{31}^0 + e_{15}^0)\frac{\partial^2 \phi}{\partial z \partial x} + c_{44}^0\frac{\partial^2 u_x}{\partial z^2}\\
&+\upsilon\left[c_{44}^0\left(\frac{\partial u_z}{\partial x} + \frac{\partial u_x}{\partial z}\right) + e_{15}^0\frac{\partial \phi}{\partial x}\right] = \rho_0\frac{\partial^2 u_x}{\partial t^2},
\end{aligned} \quad (4)$$

$$\begin{aligned}
&c_{44}^0\frac{\partial^2 u_z}{\partial x^2} + \left(c_{13}^0 + c_{44}^0\right)\frac{\partial^2 u_x}{\partial z \partial x} + e_{33}^0\frac{\partial^2 \phi}{\partial z^2} + e_{15}^0\frac{\partial^2 \phi}{\partial x^2} + c_{33}^0\frac{\partial^2 u_z}{\partial z^2}\\
&+\upsilon\left[c_{33}^0\frac{\partial u_z}{\partial z} + c_{13}^0\frac{\partial u_x}{\partial x} + e_{33}^0\frac{\partial \phi}{\partial z}\right] = \rho_0\frac{\partial^2 u_z}{\partial t^2},
\end{aligned} \quad (5)$$

$$\begin{aligned}
&e_{15}^0\frac{\partial^2 u_z}{\partial x^2} + \left(e_{15}^0 + e_{31}^0\right)\frac{\partial^2 u_x}{\partial z \partial x} + e_{33}^0\frac{\partial^2 u_z}{\partial z^2} - \varepsilon_{33}^0\frac{\partial^2 \phi}{\partial z^2} - \varepsilon_{11}^0\frac{\partial^2 \phi}{\partial x^2}\\
&+\upsilon\left[e_{33}^0\frac{\partial u_z}{\partial z} + e_{31}^0\frac{\partial u_x}{\partial x} - \varepsilon_{33}^0\frac{\partial \phi}{\partial z}\right] = 0.
\end{aligned} \quad (6)$$

The mechanical and electrical boundary conditions at $z = \varepsilon h(x)$ due to a line load (F) moving with uniform velocity V in positive direction of x-axis may be identified as

$$\tau_{xz} = -FR\delta(x - Vt) = -\frac{FR}{\pi}\int_0^\infty \cos k(x - Vt)dk, \quad (7)$$

$$\tau_{zz} = -F\delta(x - Vt) = -\frac{F}{\pi}\int_0^\infty \cos k(x - Vt)dk, \quad (8)$$

$$D_z(x) = 0 \quad \text{(for electrical open case)}, \quad (9)$$

$$\phi(x) = 0 \quad \text{(for electrical short case)}, \quad (10)$$

where newly introduced symbols k, t, R and $\delta(x)$ in Eqs. (7)-(10) represent wave number, time, frictional coefficient and Dirac delta function respectively.

Keeping in mind that displacements are bounded at $z \to \infty$, the solution of the Eqs. (4)-(6) may be considered in the following form (Chattopadhyay *et al.* 2011)

$$u_x = \int_0^\infty \left[Ae^{-kqz}\cos k(x - Vt) + Be^{-kqz}\sin k(x - Vt)\right]dk, \quad (11)$$

$$u_z = \int_0^\infty \left[Ce^{-kqz}\cos k(x - Vt) + De^{-kqz}\sin k(x - Vt)\right]dk, \quad (12)$$

$$\phi = \int_0^\infty \left[Ee^{-kqz}\cos k(x - Vt) + Fe^{-kqz}\sin k(x - Vt)\right]dk. \quad (13)$$

where A, B, C, D, E and F are unknown parameters to be obtained and q is a positive real unknown dimensionless parameter independent of k.

With aid of Eqs. (11)-(13), Eqs. (4)-(6) provide the following set of simultaneous equations

$$Aa - Db - Fc = 0,\ Ba + Cb + Ec = 0,\ Ab + Dd + Fe = 0 \quad (14)$$

$$Bb - Cd - Ee = 0,\ Bc + Ce_{15}^0 - E\varepsilon_{11}^0 = 0, \quad (15)$$

$$Ac - De_{15}^0 + F\varepsilon_{11}^0 = 0,$$

$$-Ce_{33}^0 + E\varepsilon_{33}^0 = 0,\ De_{33}^0 - F\varepsilon_{33}^0 = 0, \tag{16}$$

where the values of a, b, c, d and e are provided in Appendix A.

Now in view of setting $D = mA,\ C = -mB, E = mA\gamma$ and $F = -mB\gamma$, Eqs. (14)-(16) yield

$$m = \frac{a}{b + \gamma c} = \frac{-b}{d + \gamma e} = \frac{c}{e_{15}^0 - \gamma\varepsilon_{11}^0}. \tag{17}$$

where $\gamma = \dfrac{e_{33}^0}{\varepsilon_{33}^0}$.

Eq. (17) further leads to a biquadratic equation which has the solution in the following form

$$q_i^2 = \frac{-B' \pm \sqrt{B'^2 - 4A'C'}}{2B'} \left(\text{where } i = 1,\ 2\right). \tag{18}$$

where the expressions of A', B' and C' are given in the Appendix A.

Using Eqs. (17) and (18), the expressions of u_x, u_z and ϕ may be written as

$$u_x = \int_0^\infty \Big[A_1 e^{-kq_1 z}\cos k(x - Vt) + A_2 e^{-kq_2 z}\cos k(x - Vt) + B_1 e^{-kq_1 z}\sin k(x - Vt) + B_2 e^{-kq_2 z}\sin k(x - Vt)\Big]\, dk, \tag{19}$$

$$u_z = \int_0^\infty \Big[-m_1 B_1 e^{-kq_1 z}\cos k(x - Vt) - m_2 B_2 e^{-kq_2 z}\cos k(x - Vt) + m_1 A_1 e^{-kq_1 z}\sin k(x - Vt) + m_2 A_2 e^{-kq_2 z}\sin k(x - Vt)\Big] dk, \tag{20}$$

$$\phi = \int_0^\infty \gamma\Big[-m_1 B_1 e^{-kq_1 z}\cos k(x - Vt) - m_2 B_2 e^{-kq_2 z}\cos k(x - Vt) + m_1 A_1 e^{-kq_1 z}\sin k(x - Vt) + m_2 A_2 e^{-kq_2 z}\sin k(x - Vt)\Big]\, dk. \tag{21}$$

Since the irregularity at the surface boundary of the considered stratum is such that perturbation parameter ε is very small, therefore, the terms A_1, A_2, B_1 and B_2 can be expressed as functions of ε (expanded in ascending powers of ε and retaining up to first order by neglecting higher powers of ε) as

$$A_1 = A_{10} + \varepsilon A_{11}, A_2 = A_{20} + \varepsilon A_{21}, B_1 = B_{10} + \varepsilon B_{11},\ B_2 = B_{20} + \varepsilon B_{21} \text{ and } e^{\pm\varepsilon kh} \cong 1 \pm \varepsilon kh. \tag{22}$$

2.1 Case 1: For electrically open condition

In view of Eq. (3), boundary conditions indicated in (7-9), approximation indicated in (22) and Eqs. (19)-(21), the following system of equations can be obtained:

$$\begin{aligned} B_{10}\xi_3 + B_{20}\xi_4 &= 0, \\ B_{11}\xi_3 + B_{21}\xi_4 &= B_{10}\xi_3 kq_1 h + B_{20}\xi_4 kq_2 h, \end{aligned} \tag{23}$$

$$A_{10}\xi_3 + A_{20}\xi_4 = \frac{-FR}{\pi k},\ A_{10}\xi_1 + A_{20}\xi_2 = 0, \tag{24}$$

$$A_{11}\xi_3 + A_{21}\xi_4 = A_{10}\xi_3 h(kq_1 - \upsilon) + A_{20}\xi_4 h(kq_2 - \upsilon), \tag{25}$$

$$A_{11}\xi_1 + A_{21}\xi_2 = A_{10}\xi_1 kq_1 h + A_{20}\xi_2 kq_2 h, \tag{26}$$

$$B_{10}\xi_1 + B_{20}\xi_2 = \frac{-F}{\pi k}, \tag{27}$$

$$B_{11}\xi_1 + B_{21}\xi_2 = B_{10}\xi_1 h(kq_1 - \upsilon) + B_{20}\xi_2 h(kq_2 - \upsilon), \tag{28}$$

where the values of ξ_1, ξ_2, ξ_3 and ξ_4 are provided in Appendix A.

On solving the system of Eqs. (23)-(28), the arbitrary coefficients $A_{10}, A_{11}, A_{20}, A_{21}, B_{10}, B_{11}, B_{20}$ and B_{21} can be determined. Now, in view of these values of arbitrary coefficients, and approximation (22), Eqs. (19)-(21) yield

$$\begin{aligned} u_x = \int_0^\infty \Bigg[&\left(-\frac{\xi_2 FR}{\pi k\xi_7} - \varepsilon\frac{\xi_2 FRh}{\pi k\xi_7}(kq_1 - \upsilon)\right) e^{-kq_1 z}\cos k(x - Vt) + \\ &\left(\frac{\xi_1 FR}{\pi k\xi_7} + \varepsilon\frac{\xi_1 FRh}{\pi k\xi_7}(kq_2 - \upsilon)\right) e^{-kq_2 z}\cos k(x - Vt) + \Bigg] dk \\ &\left(\frac{\xi_4 F}{\pi k\xi_7} + \varepsilon\frac{\xi_4 Fh}{\pi k\xi_7}(kq_1 - \upsilon)\right) e^{-kq_1 z}\sin k(x - Vt) + \\ &\left(-\frac{\xi_3 F}{\pi k\xi_7} - \varepsilon\frac{\xi_3 Fh}{\pi k\xi_7}(kq_2 - \upsilon)\right) e^{-kq_2 z}\sin k(x - Vt), \end{aligned} \tag{29}$$

$$\begin{aligned} u_z = \int_0^\infty \Bigg[&m_1\left(-\frac{\xi_4 F}{\pi k\xi_7} - \varepsilon\frac{\xi_4 Fh}{\pi k\xi_7}(kq_1 - \upsilon)\right) e^{-kq_1 z}\cos k(x - Vt) + \\ &m_2\left(\frac{\xi_3 F}{\pi k\xi_7} + \varepsilon\frac{\xi_3 Fh}{\pi k\xi_7}(kq_2 - \upsilon)\right) e^{-kq_2 z}\cos k(x - Vt) + \\ &m_1\left(-\frac{\xi_2 FR}{\pi k\xi_7} - \varepsilon\frac{\xi_2 FRh}{\pi k\xi_7}(kq_1 - \upsilon)\right) e^{-kq_1 z}\sin k(x - Vt) + \\ &m_2\left(\frac{\xi_1 FR}{\pi k\xi_7} + \varepsilon\frac{\xi_1 FRh}{\pi k\xi_7}(kq_2 - \upsilon)\right) e^{-kq_2 z}\sin k(x - Vt) dk \Bigg], \end{aligned} \tag{30}$$

$$\begin{aligned} \phi = \int_0^\infty \gamma\Bigg[&m_1\left(-\frac{\xi_4 F}{\pi k\xi_7} - \varepsilon\frac{\xi_4 Fh}{\pi k\xi_7}(kq_1 - \upsilon)\right) e^{-kq_1 z}\cos k(x - Vt) \\ &+ m_2\left(\frac{\xi_3 F}{\pi k\xi_7} + \varepsilon\frac{\xi_3 Fh}{\pi k\xi_7}(kq_2 - \upsilon)\right) e^{-kq_2 z}\cos k(x - Vt) \\ &+ m_1\left(-\frac{\xi_2 FR}{\pi k\xi_7} - \varepsilon\frac{\xi_2 FRh}{\pi k\xi_7}(kq_1 - \upsilon)\right) e^{-kq_1 z}\sin k(x - Vt) \\ &+ m_2\left(\frac{\xi_1 FR}{\pi k\xi_7} + \varepsilon\frac{\xi_1 FRh}{\pi k\xi_7}(kq_2 - \upsilon)\right) e^{-kq_2 z}\sin k(x - Vt) \Bigg] dk. \end{aligned} \tag{31}$$

On substituting the values of u_x, u_z and ϕ from Eqs. (29)-(31) into Eq. (3) and performing integration, the expressions of induced compressive stress $\left(\tau_{zz}/F\right)$, shear stress $\left(\tau_{zx}/F\right)$, tensile stress $\left(\tau_{xx}/F\right)$, vertical electrical displacement $\left(D_z/F\right)$ and horizontal electrical displacement $\left(D_x/F\right)$ may be obtained for electrically open case in the said geometry as

$$\frac{\tau_{zz}}{F}=\frac{e^{\upsilon z}\xi_1}{\pi\xi_7 s_1^2}\Big[\xi_4 q_1^3 z^3+\varepsilon h\xi_4 q_1^3 z^2+R\xi_2 q_1^2(x-Vt)z^2+2R\varepsilon h\xi_2 q_1^2(x-Vt)z$$
$$+\xi_4 q_1(x-Vt)^2 z-\varepsilon h\xi_4 q_1(x-Vt)^2+R\xi_2(x-Vt)^3-\varepsilon h\xi_4\upsilon q_1^3 z^2$$
$$-R\varepsilon h\xi_2\upsilon(x-Vt)^3-R\varepsilon h\xi_2 q_1^2\upsilon(x-Vt)z^2-\varepsilon h\xi_4 q_1\upsilon(x-Vt)^2 z\Big]$$
$$-\frac{e^{\upsilon z}\xi_2}{\pi\xi_7 s_2^2}\Big[\xi_3 q_2^3 z^3+\varepsilon h\xi_3 q_2^3 z^2+R\xi_1 q_2^2(x-Vt)z^2+2R\varepsilon h\xi_1 q_2^2(x-Vt)z \quad (32)$$
$$+\xi_3 q_2(x-Vt)^2 z-\varepsilon h\xi_3 q_2(x-Vt)^2+R\xi_1(x-Vt)^3-\varepsilon h\xi_3\upsilon q_2^3 z^2$$
$$-R\varepsilon h\xi_1 q_2^2\upsilon(x-Vt)z^2-\varepsilon h\xi_3 q_2\upsilon(x-Vt)^2 z-R\varepsilon h\xi_1\upsilon(x-Vt)^3\Big],$$

$$\frac{\tau_{zx}}{F}=\frac{e^{\upsilon z}\xi_3}{\pi\xi_7 s_1^2}\Big[-R\xi_2 q_1^3 z^3-R\varepsilon h\xi_2 q_1^3 z^2+\xi_4 q_1^2(x-Vt)z^2$$
$$+2\varepsilon h\xi_4 q_1^2(x-Vt)z-R\xi_2 q_1(x-Vt)^2 z+R\varepsilon h\xi_2 q_1(x-Vt)^2$$
$$+\xi_4(x-Vt)^3+R\varepsilon h\xi_2\upsilon q_1^3 z^2-\varepsilon h\xi_4 q_1^2\upsilon(x-Vt)z^2$$
$$+R\varepsilon h\xi_2 q_1\upsilon(x-Vt)^2 z-\varepsilon h\xi_2\upsilon(x-Vt)^3\Big]-\frac{e^{\upsilon z}\xi_4}{\pi\xi_7 s_2^2}\Big[-R\xi_1 q_2^3 z^3 \quad (33)$$
$$-R\varepsilon h\xi_1 q_2^3 z^2+\xi_3 q_2^2(x-Vt)z^2+2\varepsilon h\xi_3 q_2^2(x-Vt)z$$
$$-R\xi_1 q_2(x-Vt)^2 z+R\varepsilon h\xi_1 q_2(x-Vt)^2+\xi_3(x-Vt)^3+R\varepsilon h\xi_1\upsilon q_2^3 z^2$$
$$-\varepsilon h\xi_3 q_2^2\upsilon(x-Vt)z^2+R\varepsilon h\xi_1 q_2\upsilon(x-Vt)^2 z-\varepsilon h\xi_3\upsilon(x-Vt)^3\Big],$$

$$\frac{\tau_{xx}}{F}=\frac{e^{\upsilon z}\xi_8}{\pi\xi_7 s_1^2}\Big[\xi_4 q_1^3 z^3+\varepsilon h\xi_4 q_1^3 z^2+R\xi_2 q_1^2(x-Vt)z^2$$
$$+2R\varepsilon h\xi_2 q_1^2(x-Vt)z+\xi_4 q_1(x-Vt)^2 z-\varepsilon h\xi_4 q_1(x-Vt)^2$$
$$+R\xi_2(x-Vt)^3-\varepsilon h\xi_4\upsilon q_1^3 z^2-R\varepsilon h\xi_2\upsilon(x-Vt)^3$$
$$-R\varepsilon h\xi_2 q_1^2\upsilon(x-Vt)z^2-\varepsilon h\xi_4 q_1\upsilon(x-Vt)^2 z\Big]- \quad (34)$$
$$\frac{e^{\upsilon z}\xi_9}{\pi\xi_7 s_2^2}\Big[\xi_3 q_2^3 z^3+\varepsilon h\xi_3 q_2^3 z^2+R\xi_1 q_2^2(x-Vt)z^2+2R\varepsilon h\xi_1 q_2^2(x-Vt)z$$
$$+\xi_3 q_2(x-Vt)^2 z-\varepsilon h\xi_3 q_2(x-Vt)^2+R\xi_1(x-Vt)^3-\varepsilon h\xi_3\upsilon q_2^3 z^2$$
$$-R\varepsilon h\xi_1 q_2^2\upsilon(x-Vt)z^2-\varepsilon h\xi_3 q_2\upsilon(x-Vt)^2 z-R\varepsilon h\xi_1\upsilon(x-Vt)^3\Big],$$

$$\frac{D_z}{F}=-\frac{e^{\upsilon z}\xi_5}{\pi\xi_7 s_1^2}\Big[\xi_4 q_1^3 z^3+\varepsilon h\xi_4 q_1^3 z^2+R\xi_2 q_1^2(x-Vt)z^2$$
$$+2R\varepsilon h\xi_2 q_1^2(x-Vt)z+\xi_4 q_1(x-Vt)^2 z-\varepsilon h\xi_4 q_1(x-Vt)^2$$
$$+R\xi_2(x-Vt)^3-\varepsilon h\xi_4\upsilon q_1^3 z^2-R\varepsilon h\xi_2 q_1^2\upsilon(x-Vt)z^2$$
$$-\varepsilon h\xi_4 q_1\upsilon(x-Vt)^2 z-R\varepsilon h\xi_2\upsilon(x-Vt)^3+\frac{e^{\upsilon z}\xi_6}{\pi\xi_7 s_2^2}\Big[\xi_3 q_2^3 z^3 \quad (35)$$
$$+\varepsilon h\xi_3 q_2^3 z^2+R\xi_1 q_2^2(x-Vt)z^2+2R\varepsilon h\xi_1 q_2^2(x-Vt)z+$$
$$\xi_3 q_2(x-Vt)^2 z-\varepsilon h\xi_3 q_2(x-Vt)^2+R\xi_1(x-Vt)^3-\varepsilon h\xi_3\upsilon q_2^3 z^2$$
$$-R\varepsilon h\xi_1 q_2^2\upsilon(x-Vt)z^2-\varepsilon h\xi_3 q_2\upsilon(x-Vt)^2 z-R\varepsilon h\xi_1\upsilon(x-Vt)^3\Big],$$

$$\frac{D_x}{F}=\frac{e^{\upsilon z}\xi_{10}}{\pi\xi_7 s_1^2}\Big[-R\xi_2 q_1^3 z^3-R\varepsilon h\xi_2 q_1^3 z^2+\xi_4 q_1^2(x-Vt)z^2$$
$$+2\varepsilon h\xi_2 q_1^2(x-Vt)z-R\xi_2 q_1(x-Vt)^2 z+R\varepsilon h\xi_2 q_1(x-Vt)^2$$
$$+\xi_4(x-Vt)^3+R\varepsilon h\xi_2\upsilon q_1^3 z^2-\varepsilon h\xi_4 q_1^2\upsilon(x-Vt)z^2$$
$$+R\varepsilon h\xi_2 q_1\upsilon(x-Vt)^2 z-\varepsilon h\xi_2\upsilon(x-Vt)^3\Big]-\frac{e^{\upsilon z}\xi_{11}}{\pi\xi_7 s_2^2}\Big[-R\xi_1 q_2^3 z^3 \quad (36)$$
$$-R\varepsilon h\xi_1 q_2^3 z^2+\xi_3 q_2^2(x-Vt)z^2+2\varepsilon h\xi_3 q_2^2(x-Vt)z$$
$$-R\xi_1 q_2(x-Vt)^2 z+R\varepsilon h\xi_1 q_2(x-Vt)^2+\xi_3(x-Vt)^3$$
$$+R\varepsilon h\xi_1\upsilon q_2^3 z^2-\varepsilon h\xi_3 q_2^2\upsilon(x-Vt)z^2+R\varepsilon h\xi_1 q_2\upsilon(x-Vt)^2 z$$
$$-\varepsilon h\xi_3\upsilon(x-Vt)^3\Big].$$

where the values of $\xi_r\,(r=1,2,3.....10,11)$ are provided in Appendix A.

2.2 Case 2: For electrically short condition

On using Eq. (3), boundary conditions indicated in (7), (8), and (10); approximation indicated in (22) and Eqs. (19)-(21), the following system of equations can be obtained

$$B_{10}\xi_3'+B_{20}\xi_4'=0,\ B_{11}\xi_3'+B_{21}\xi_4'=B_{10}\xi_3' kq_1 h+B_{20}\xi_4' kq_2 h, \quad (37)$$

$$A_{10}\xi_3'+A_{20}\xi_4'=\frac{-FR}{\pi k},\ A_{10}\xi_1'+A_{20}\xi_2'=0, \quad (38)$$

$$A_{11}\xi_3'+A_{21}\xi_4'=A_{10}\xi_3' h(kq_1-\upsilon)+A_{20}\xi_4' h(kq_2-\upsilon), \quad (39)$$

$$A_{11}\xi_1'+A_{21}\xi_2'=A_{10}\xi_1' kq_1 h+A_{20}\xi_2' kq_2 h,$$
$$B_{10}\xi_1'+B_{20}\xi_2'=\frac{-F}{\pi k}, \quad (40)$$

$$B_{11}\xi_1'+B_{21}\xi_2'=B_{10}\xi_1' h(kq_1-\upsilon)+B_{20}\xi_2' h(kq_2-\upsilon), \quad (41)$$

where the values of $\xi_1', \xi_2', \xi_3', \text{and}\,\xi_4'$ are provided in Appendix A.

The arbitrary coefficients $A_{10}, A_{11}, A_{20}, A_{21}, B_{10}, B_{11}, B_{20}$ and B_{21} can be determined by solving system of Eqs. (37)-(41). With aid of obtained values of arbitrary coefficients and approximation (22), Eqs. (19)-(21) results in

$$u_x=\int_0^\infty\Big[\Big(-\frac{\xi_2'FR}{\pi k\xi_7'}-\varepsilon\frac{\xi_2'FRh}{\pi k\xi_7'}(kq_1-\upsilon)\Big)e^{-kq_1 z}\cos k(x-Vt)$$
$$+\Big(\frac{\xi_1'FR}{\pi k\xi_7'}+\varepsilon\frac{\xi_1'FRh}{\pi k\xi_7'}(kq_2-\upsilon)\Big)e^{-kq_2 z}\cos k(x-Vt)$$
$$\Big(\frac{\xi_4'F}{\pi k\xi_7'}+\varepsilon\frac{\xi_4'Fh}{\pi k\xi_7'}(kq_1-\upsilon)\Big)e^{-kq_1 z}\sin k(x-Vt)+ \quad (42)$$
$$\Big(-\frac{\xi_3'F}{\pi k\xi_7'}-\varepsilon\frac{\xi_3'Fh}{\pi k\xi_7'}(kq_2-\upsilon)\Big)e^{-kq_2 z}\sin k(x-Vt)\Big]dk,$$

$$u_z=\int_0^\infty\Big[m_1\Big(-\frac{\xi_4'F}{\pi k\xi_7'}-\varepsilon\frac{\xi_4'Fh}{\pi k\xi_7'}(kq_1-\upsilon)\Big)e^{-kq_1 z}\cos k(x-Vt)$$
$$+m_2\Big(\frac{\xi_3'F}{\pi k\xi_7'}+\varepsilon\frac{\xi_3'Fh}{\pi k\xi_7'}(kq_2-\upsilon)\Big)e^{-kq_2 z}\cos k(x-Vt)$$
$$+m_1\Big(-\frac{\xi_2'FR}{\pi k\xi_7'}-\varepsilon\frac{\xi_2'FRh}{\pi k\xi_7'}(kq_1-\upsilon)\Big)e^{-kq_1 z}\sin k(x-Vt) \quad (43)$$
$$+m_2\Big(\frac{\xi_1'FR}{\pi k\xi_7'}+\varepsilon\frac{\xi_1'FRh}{\pi k\xi_7'}(kq_2-\upsilon)\Big)e^{-kq_2 z}\sin k(x-Vt)\Big]dk,$$

$$\phi=\int_0^\infty\gamma\Big[m_1\Big(-\frac{\xi_4'F}{\pi k\xi_7'}-\varepsilon\frac{\xi_4'Fh}{\pi k\xi_7'}(kq_1-\upsilon)\Big)e^{-kq_1 z}\cos k(x-Vt)$$
$$+m_2\Big(\frac{\xi_3'F}{\pi k\xi_7'}+\varepsilon\frac{\xi_3'Fh}{\pi k\xi_7'}(kq_2-\upsilon)\Big)e^{-kq_2 z}\cos k(x-Vt)$$
$$+m_1\Big(-\frac{\xi_2'FR}{\pi k\xi_7'}-\varepsilon\frac{\xi_2'FRh}{\pi k\xi_7'}(kq_1-\upsilon)\Big)e^{-kq_1 z}\sin k(x-Vt) \quad (44)$$
$$+m_2\Big(\frac{\xi_1'FR}{\pi k\xi_7'}+\varepsilon\frac{\xi_1'FRh}{\pi k\xi_7'}(kq_2-\upsilon)\Big)e^{-kq_2 z}\sin k(x-Vt)\Big]dk.$$

Substituting the values of u_x, u_z and ϕ from Eqs. (42)-(44) into Eq. (3) and performing integration, the expressions of

induced compressive stress (τ_{zz}/F), shear stress (τ_{zx}/F), tensile stress (τ_{xx}/F), vertical electrical displacement (D_z/F) and horizontal electrical displacement (D_x/F) may be obtained for electrically short case in the said geometry as

$$\begin{aligned}\frac{\tau_{zz}}{F}=&\frac{e^{\upsilon z}\xi_1'}{\pi\xi_7's_1^2}\Big[\xi_4'q_1^3z^3+\varepsilon h\xi_4'q_1^3z^2+R\xi_2'q_1^2(x-Vt)z^2+2R\varepsilon h\xi_2'q_1^2(x-Vt)z\\&+\xi_4'q_1(x-Vt)^2z-\varepsilon h\xi_4'q_1(x-Vt)^2+R\xi_2'(x-Vt)^3-\varepsilon h\xi_4'\upsilon q_1^3z^2\\&-R\varepsilon h\xi_2'q_1^2\upsilon(x-Vt)z^2-\varepsilon h\xi_4'q_1\upsilon(x-Vt)^2z-R\varepsilon h\xi_2'\upsilon(x-Vt)^3\\&-\frac{e^{\upsilon z}\xi_2'}{\pi\xi_7's_2^2}\Big[\xi_3'q_2^3z^3+\varepsilon h\xi_3'q_2^3z^2+R\xi_1'q_2^2(x-Vt)z^2+2R\varepsilon h\xi_1'q_2^2(x-Vt)z\\&+\xi_3'q_2(x-Vt)^2z-\varepsilon h\xi_3'q_2(x-Vt)^2+R\xi_1'(x-Vt)^3-\varepsilon h\xi_3'\upsilon q_2^3z^2\\&-R\varepsilon h\xi_1'q_2^2\upsilon(x-Vt)z^2-\varepsilon h\xi_3'q_2\upsilon(x-Vt)^2z-R\varepsilon h\xi_1'\upsilon(x-Vt)^3\Big],\end{aligned}\tag{45}$$

$$\begin{aligned}\frac{\tau_{zx}}{F}=&\frac{e^{\upsilon z}\xi_3'}{\pi\xi_7's_1^2}\Big[-R\xi_2'q_1^3z^3-R\varepsilon h\xi_2'q_1^3z^2+\xi_4'q_1^2(x-Vt)z^2+2\varepsilon h\xi_2'q_1^2(x-Vt)z\\&-R\xi_2'q_1(x-Vt)^2z+R\varepsilon h\xi_2'q_1(x-Vt)^2+\xi_4'(x-Vt)^3+R\varepsilon h\xi_2'\upsilon q_1^3z^2\\&-\varepsilon h\xi_4'q_1^2\upsilon(x-Vt)z^2+R\varepsilon h\xi_2'q_1\upsilon(x-Vt)^2z-\varepsilon h\xi_2'\upsilon(x-Vt)^3\Big]\\&-\frac{e^{\upsilon z}\xi_4'}{\pi\xi_7's_2^2}\Big[-R\xi_1'q_2^3z^3-R\varepsilon h\xi_1'q_2^3z^2+\xi_3'q_2^2(x-Vt)z^2+2\varepsilon h\xi_3'q_2^2(x-Vt)z\\&-R\xi_1'q_2(x-Vt)^2z+R\varepsilon h\xi_1'q_2(x-Vt)^2+\xi_3'(x-Vt)^3+R\varepsilon h\xi_1'\upsilon q_2^3z^2\\&-\varepsilon h\xi_3'q_2^2\upsilon(x-Vt)z^2+R\varepsilon h\xi_1'q_2\upsilon(x-Vt)^2z-\varepsilon h\xi_3'\upsilon(x-Vt)^3\Big],\end{aligned}\tag{46}$$

$$\begin{aligned}\frac{\tau_{xx}}{F}=&\frac{e^{\upsilon z}\xi_8'}{\pi\xi_7's_1^2}\Big[\xi_4'q_1^3z^3+\varepsilon h\xi_4'q_1^3z^2+R\xi_2'q_1^2(x-Vt)z^2\\&+2R\varepsilon h\xi_2'q_1^2(x-Vt)z+\xi_4'q_1(x-Vt)^2z-\varepsilon h\xi_4'q_1(x-Vt)^2\\&+R\xi_2'(x-Vt)^3-\varepsilon h\xi_4'\upsilon q_1^3z^2-R\varepsilon h\xi_2'\upsilon(x-Vt)^3\\&-R\varepsilon h\xi_2'q_1^2\upsilon(x-Vt)z^2-\varepsilon h\xi_4'q_1\upsilon(x-Vt)^2z\Big]-\frac{e^{\upsilon z}\xi_9'}{\pi\xi_7's_2^2}\Big[\xi_3'q_2^3z^3+\\&\varepsilon h\xi_3'q_2^3z^2+R\xi_1'q_2^2(x-Vt)z^2+2R\varepsilon h\xi_1'q_2^2(x-Vt)z+\xi_3'q_2(x-Vt)^2z-\\&\varepsilon h\xi_3'q_2(x-Vt)^2+R\xi_1'(x-Vt)^3-\varepsilon h\xi_3'\upsilon q_2^3z^2-R\varepsilon h\xi_1'q_2^2\upsilon(x-Vt)z^2\\&-\varepsilon h\xi_3'q_2\upsilon(x-Vt)^2z-R\varepsilon h\xi_1'\upsilon(x-Vt)^3\Big],\end{aligned}\tag{47}$$

$$\begin{aligned}\frac{D_z}{F}=&-\frac{e^{\upsilon z}\xi_5'}{\pi\xi_7's_1^2}\Big[\xi_4'q_1^3z^3+\varepsilon h\xi_4'q_1^3z^2+R\xi_2'q_1^2(x-Vt)z^2\\&+2R\varepsilon h\xi_2'q_1^2(x-Vt)z+\xi_4'q_1(x-Vt)^2z-\varepsilon h\xi_4'q_1(x-Vt)^2\\&+R\xi_2'(x-Vt)^3-\varepsilon h\xi_4'\upsilon q_1^3z^2-\varepsilon h\xi_2'R\upsilon q_1^2(x-Vt)z^2-\varepsilon h\xi_4'q_1\upsilon(x-Vt)^2z\\&-R\varepsilon h\xi_2'\upsilon(x-Vt)^3\Big]+\frac{e^{\upsilon z}\xi_6'}{\pi\xi_7's_2^2}\Big[\xi_3'q_2^3z^3+\varepsilon h\xi_3'q_2^3z^2\\&+R\xi_1'q_2^2(x-Vt)z^2+2R\varepsilon h\xi_1'q_2^2(x-Vt)z+\xi_3'q_2(x-Vt)^2z\\&-\varepsilon h\xi_3'q_2(x-Vt)^2+R\xi_1'(x-Vt)^3-\varepsilon h\xi_3'\upsilon q_2^3z^2\\&-R\varepsilon h\xi_1'q_2^2\upsilon(x-Vt)z^2-\varepsilon h\xi_3'q_2\upsilon(x-Vt)^2z-R\varepsilon h\xi_1'\upsilon(x-Vt)^3\Big],\end{aligned}\tag{48}$$

$$\begin{aligned}\frac{D_x}{F}=&\frac{e^{\upsilon z}\xi_{10}'}{\pi\xi_7's_1^2}\Big[-R\xi_2'q_1^3z^3-R\varepsilon h\xi_2'q_1^3z^2+\xi_4'q_1^2(x-Vt)z^2\\&+2\varepsilon h\xi_2'q_1^2(x-Vt)z-R\xi_2'q_1(x-Vt)^2z+R\varepsilon h\xi_2'q_1(x-Vt)^2\\&+\xi_4'(x-Vt)^3+R\varepsilon h\xi_2'\upsilon q_1^3z^2-\varepsilon h\xi_4'q_1^2\upsilon(x-Vt)z^2+\\&R\varepsilon h\xi_2'q_1\upsilon(x-Vt)^2z-\varepsilon h\xi_2'\upsilon(x-Vt)^3-\frac{e^{\upsilon z}\xi_{11}'}{\pi\xi_7's_2^2}\Big[-R\xi_1'q_2^3z^3-R\varepsilon h\xi_1'q_2^3z^2\\&+\xi_3'q_2^2(x-Vt)z^2+2\varepsilon h\xi_3'q_2^2(x-Vt)z-R\xi_1'q_2(x-Vt)^2z\\&+R\varepsilon h\xi_1'q_2(x-Vt)^2+\xi_3'(x-Vt)^3+\\&R\varepsilon h\xi_1'\upsilon q_2^3z^2-\varepsilon h\xi_3'q_2^2\upsilon(x-Vt)z^2+R\varepsilon h\xi_1'q_2\upsilon(x-Vt)^2z\\&-\varepsilon h\xi_3'\upsilon(x-Vt)^3\Big],\end{aligned}\tag{49}$$

where the values of $\xi_r'\,(r=1,2,3.....10,11)$ are provided in Appendix A.

The expressions in Eqs. (32)-(36) and Eqs. (45)-(49) include closed form expressions of induced incremental compressive stress, shear stress, tensile stress, vertical electrical displacement and horizontal electrical displacement for electrically open condition and electrically short condition respectively. From above expressions of induced incremental stresses and electrical displacements, it is clear that the whole system is moving with uniform velocity V in the direction of positive x-axis. It has also been observed from closed form expressions that said induced incremental stresses and electrical displacements attain maximum value at $x=Vt$ .i.e. the point directly below the point of application of moving load. In further computation, the authors deal with these maximum incremental induced stresses and electrical displacements for both electrically open and short conditions.

3. Particular case

When $c_{11}^0=c_{33}^0=(\lambda+2\mu)$, $c_{13}^0=\lambda$, $c_{44}^0=c_{66}^0=\mu$, $\varepsilon=0$, $e_{15}^0=e_{31}^0=\varepsilon_{11}^0=\varepsilon_{33}^0=0$ and $\upsilon=0$, the expressions for induced incremental mechanical stresses and induced electrical displacements for both electrically open and short conditions reduce to

$$\frac{\tau_{zz}}{F}=\frac{1}{\pi\xi_7''}\left(\frac{\xi_1''\xi_4''}{q_1'z}-\frac{\xi_2''\xi_3''}{q_2'z}\right),\tag{50}$$

$$\frac{\tau_{zx}}{F}=\frac{1}{\pi\xi_7''}\left(-\frac{R\xi_3''\xi_2''}{q_1'z}+\frac{R\xi_4''\xi_1''}{q_2'z}\right),\tag{51}$$

$$\frac{\tau_{xx}}{F}=\frac{1}{\pi\xi_7''}\left(\frac{\xi_8''\xi_4''}{q_1'z}-\frac{\xi_9''\xi_3''}{q_2'z}\right),\tag{52}$$

$$\frac{D_z}{F}=0,\quad \frac{D_x}{F}=0.\tag{53}$$

where the values of ξ_1'', ξ_2'', ξ_3'', ξ_4'', ξ_7'', ξ_8'', and ξ_9'' are provided in Appendix B.

The expressions in Eqs. (50)-(52) signify the incremental mechanical stresses induced in regular homogeneous isotropic elastic medium. These expressions are found to be well in agreement with the pre-established results by Cole and Huth (1958).

4. Numerical results and discussion

The numerical computations of incremental induced compressive stress $(\tau_{zz}a_1/F)$, induced shear stress $(\tau_{zx}a_1/F)$, induced tensile stress $(\tau_{xx}a_1/F)$, horizontal electrical displacement (D_x/F) and vertical electrical displacement

(D_z / F) have been accomplished using the following values of elastic, piezoelectric and dielectric constants of transversely isotropic piezoelectric material and elastic constants of transversely isotropic non-piezoelectric material (Table 1)

Graphical illustrations of induced maximum incremental compressive stress $(\tau_{zz} a_1 / F)$, shear stress $(\tau_{zx} a_1 / F)$, tensile stress $(\tau_{xx} a_1 / F)$, vertical electrical displacement (D_z / F), horizontal electrical displacement (D_x / F) against vertical depth have been carried out using Figs. 2(a) to 10(a). The effect of various affecting parameters viz. maximum depth of irregularity (H / a_1), irregularity factor (x / a_1) and parameter of functionally gradedness (υa_1) on induced compressive stress, shear stress, tensile stress, vertical electrical displacement and horizontal electrical displacement due to a moving load on an irregular transversely isotropic FGPM substrate $(PZT-4)$ have been manifested through Figs. 2(a) to 6(b). In these figures, curves 1, 2 and 3 delineate the effect of maximum depth of irregularity on the said induced stresses and induced electrical displacements. Curve 1 corresponds to the situation when the irregularity is absent in the considered substrate.

Table 1 Elastic, piezoelectric and dielectric constants of transversely isotropic piezoelectric materials and elastic constants of transversely isotropic non-piezoelectric material (Sridhar *et al.* 1999, Payton 2012)

Property	Unit	$PZT-4$	$(Ba_{0.917}Ca_{0.083})TiO_3$	Cadmium
Density (ρ)	kg/m^3	7500	5700	8700
Elastic Constants				
c_{11}^0	GPa	13.9	15.8	11.6
c_{13}^0	GPa	7.43	6.75	4.14
c_{33}^0	GPa	11.5	15	5.10
c_{44}^0	GPa	2.56	4.5	1.95
Dielectric constants				
ε_{11}^0	nF/m	6.461	8.850	---
ε_{33}^0	nF/m	5.620	8.054	
Piezoelectric Constants				
e_{11}^0	c/m^2	–5.2	–3.1	---
e_{33}^0	c/m^2	15.1	13.5	
e_{15}^0	c/m^2	12.7	10.9	

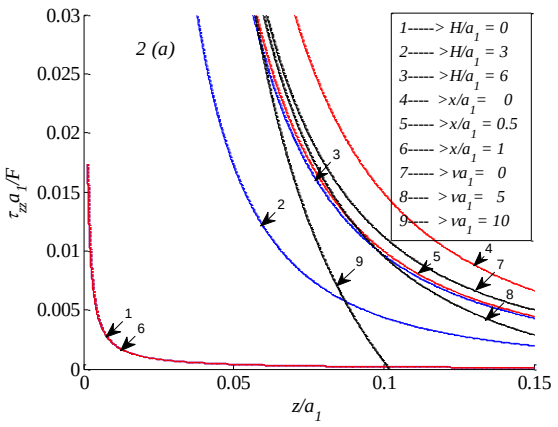

(a) Electrically open condition

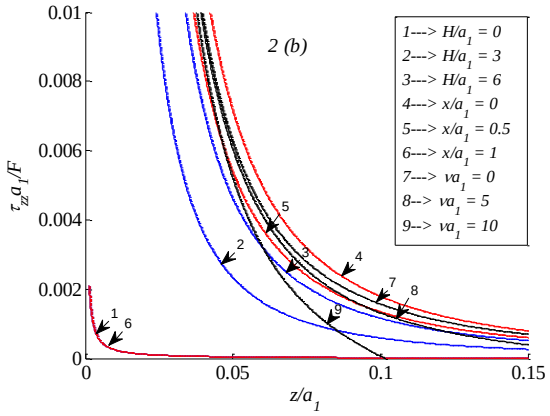

(b) Electrically short condition

Fig. 2 Variation of dimensionless induced compressive stress $(\tau_{zz} a_1 / F)$ against dimensionless vertical depth (z / a_1) for different values of dimensionless maximum depth of irregularity (H / a_1), dimensionless irregularity factor (x / a_1) and dimensionless parameter of functionally gradedness (υa_1).

The influence of irregularity in terms of irregularity factor on the said induced stresses and induced electrical displacements has been depicted by the curves 4, 5 and 6. In particular, curve 4 corresponds to the irregularity factor $x / a_1 = 0$ which represents the case of rectangular shaped irregularity on the surface of substrate. Curve 5 reveals the case of parabolic shaped irregularity $(0 < x / a_1 < 1)$ while curve 6 depicts the case of no irregularity $(x / a_1 = 1)$ exists on the surface of substrate. Moreover, the effect of parameter of functionally gradedness on said induced incremental stresses and electrical displacements has been analysed through the curves 7, 8 and 9. Among these curves, curve 7 corresponds to the situation when irregular substrate is free from functional gradient property.

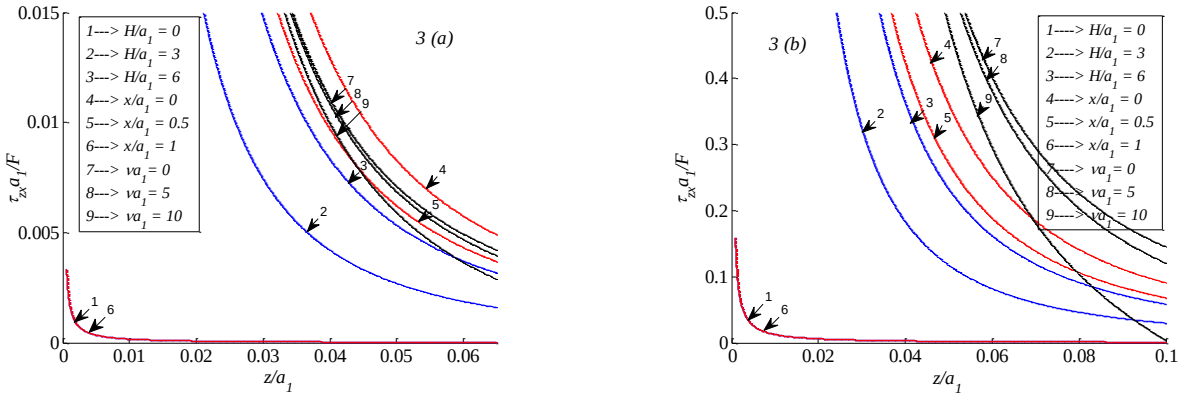

(a) Electrically open condition (b) Electrically short condition

Fig. 3 Variation of dimensionless induced shear stress $(\tau_{zx}a_1/F)$ against dimensionless vertical depth for different values of dimensionless maximum depth of irregularity, dimensionless irregularity factor and dimensionless parameter of functionally gradedness

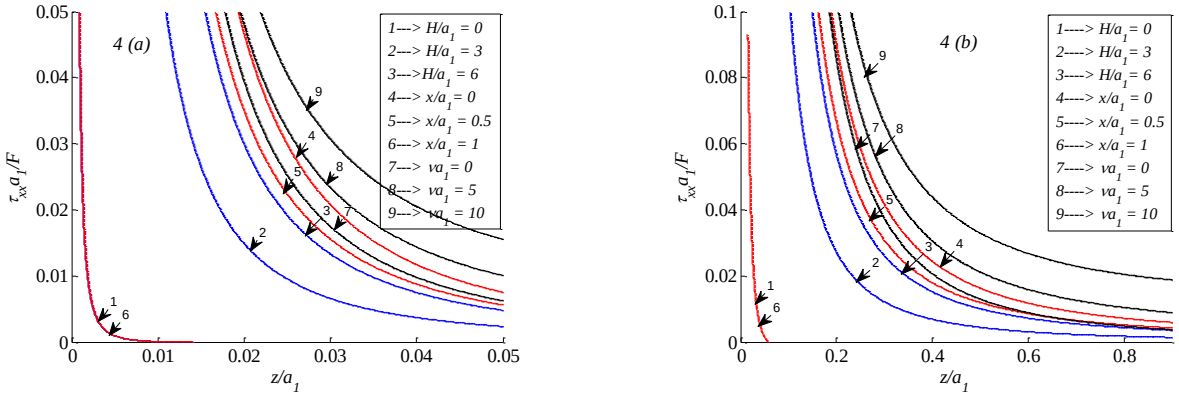

(a) Electrically open condition (b) Electrically short condition

Fig. 4 Variation of dimensionless induced tensile stress $(\tau_{xx}a_1/F)$ against dimensionless vertical depth for different values of dimensionless maximum depth of irregularity, dimensionless irregularity factor and dimensionless parameter of functionally gradedness.

Figs. 2(a) and 2(b) represent the variation of incremental induced compressive stress against vertical depth under the influence of various affecting parameters viz. maximum depth of irregularity, irregularity factor and parameter of functionally gradedness for electrically open condition and electrically short condition respectively. It has been examined from these figures that the induced compressive stress is found to be minimum in absence of irregularity and it increases as the maximum depth of irregularity increases for both electrically open and short conditions. Further, it has been observed that as the irregularity factor increases i.e., irregularity decreases, the induced compressive stress also decreases for both electrically open and short conditions. Moreover, it is also noticed that as parameter of functional gradedness increases, induced compressive stress decreases i.e., functional gradient property in the substrate affected adversely the induced compressive stress for both electrically open condition and short condition.

Figs. 3(a) and 3(b) reveal the effect of maximum depth of irregularity, irregularity factor and parameter of functionally gradedness on induced shear stress for both electrically open and short conditions respectively. It has been observed from these figures that maximum depth of irregularity favours the induced shear stress while irregularity factor and parameter of functionally gradedness exhibit an adverse effect on induced shear stress in considered piezoelectric substrate for both electrically open and short conditions. The variation of induced tensile stress against vertical depth for electrically open and short conditions under the influence of aforesaid affecting parameters has been graphically demonstrated in Figs. 4(a) and 4(b). It has been found through meticulous examination of these figures that maximum depth of irregularity and functionally gradedness favours the induced tensile stress while irregularity factor affected adversely the induced tensile stress irrespective of electrically open or short

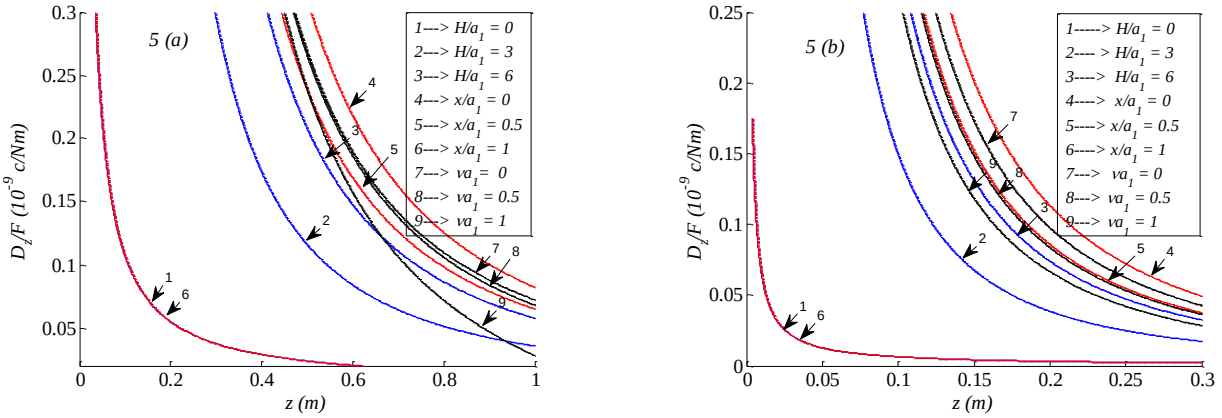

(a) Electrically open condition (b) Electrically short condition

Fig. 5 Variation of vertical electrical displacement (D_z / F) against vertical depth (z) for different values of maximum depth of irregularity, irregularity factor and parameter of functionally gradedness

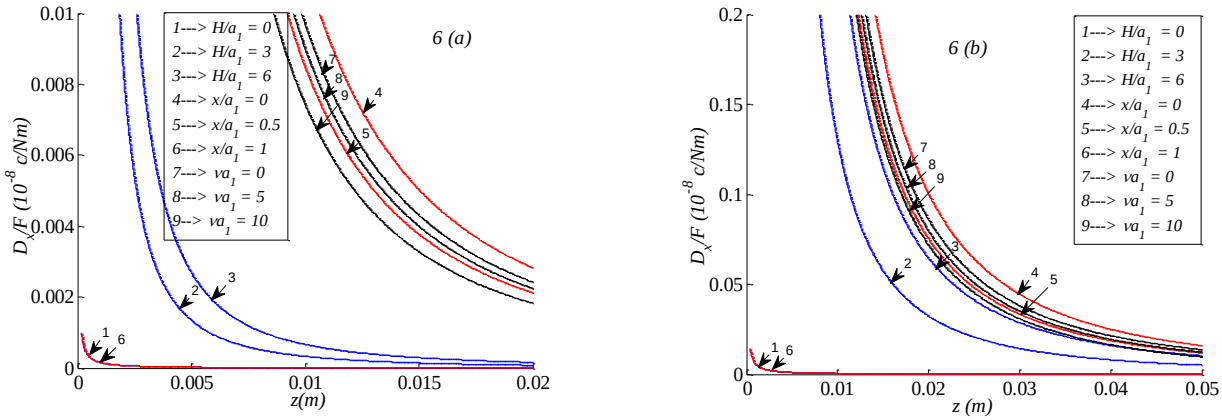

(a) Electrically open condition (b) Electrically short condition

Fig. 6 Variation of horizontal electrical displacement (D_x / F) against vertical depth (z) for different values of maximum depth of irregularity, irregularity factor and parameter of functionally gradedness

conditions on piezoelectric substrate. The effect of said affecting parameters on induced vertical electrical displacement has been depicted through Figs. 5(a) and 5(b) for electrically open and short conditions respectively. It is indicated through these figures that as the maximum depth of irregularity increases the vertical electrical displacement induced due to a moving load on considered piezoelectric substrate increases gradually for both electrically open and short conditions. It has also been examined from Figs. 5(a) and 5(b) that surface irregularity favours the induced vertical electrical displacement. In addition, the functional gradient property in piezoelectric substrate has remarkable influence on induced vertical electrical displacement. It has been examined from both the figures that as the functional gradient property prevails in the substrate the vertical electrical displacement decreases gradually irrespective of electrically open or short conditions. On the other hand, the influences of said affecting parameters on horizontal electrical displacement for electrically open and short conditions have been studied through Figs. 6(a) and 6(b) respectively. It has been delineated from both the figures that maximum depth of irregularity favours the horizontal electrical displacement while functionally gradedness and irregularity factor discourage induced vertical electrical displacement due to a moving load. The effect of frictional coefficient (R) on induced shear stress and horizontal electrical displacement due to a moving load on an irregular transversely isotropic FGPM substrate $(PZT-4)$ for both electrically open condition (through curves 1, 2, 3) and electrically short condition (through curves 4, 5, 6) in Figs. 7(a) and 7(b) respectively. Specifically, Fig. 7(a) reflects the influence of frictional coefficient on induced shear stress for both electrically open and short conditions. It has been observed from this figure that as the frictional coefficient increases the induced shear stresses also gradually increases. The effect of frictional coefficient on induced horizontal electrical displacement has been studied

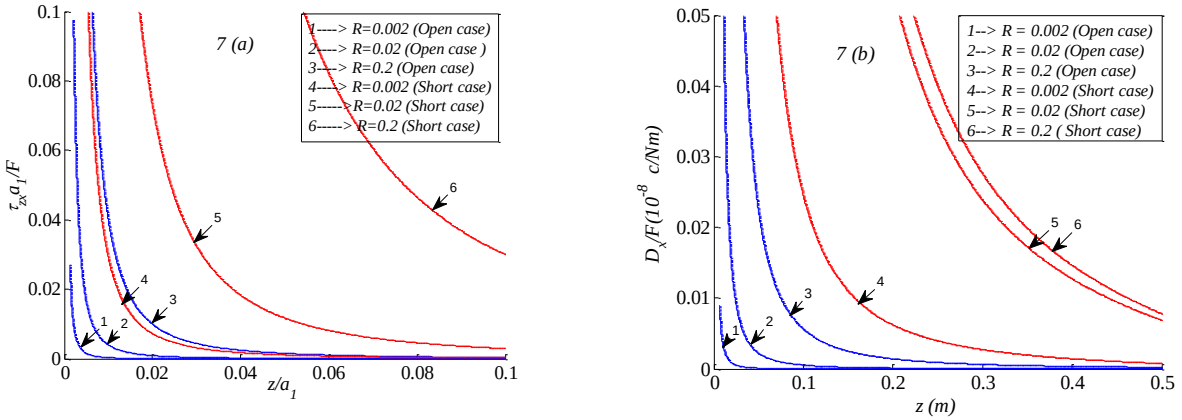

Fig. 7 Variation of (a) dimensionless induced shear stress $(\tau_{zx}a_1/F)$ against dimensionless vertical depth (z/a_1) (b) horizontal electrical displacement (D_x/F) against vertical depth (z) for different values of frictional coefficient (R).

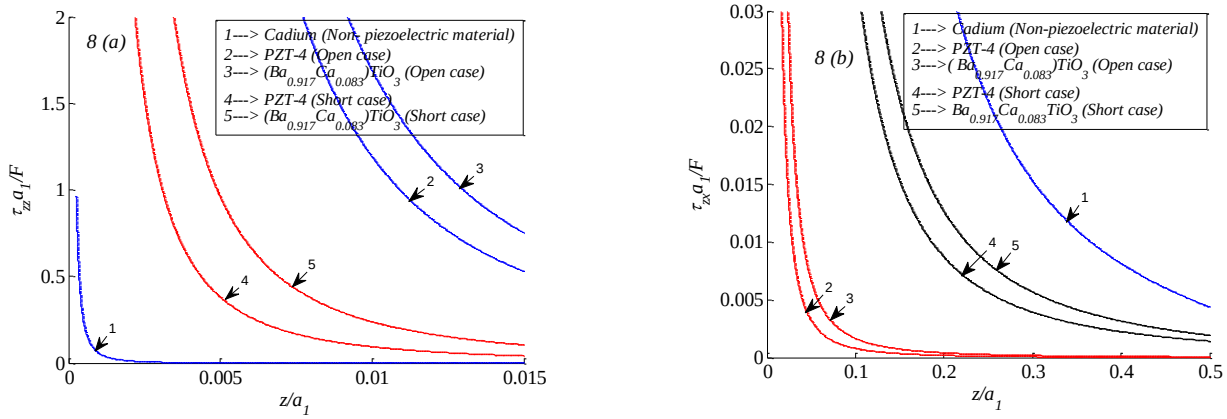

Fig. 8 Variation of (a) dimensionless induced compressive stress $(\tau_{zz}a_1/F)$ (b) dimensionless induced shear stress $(\tau_{zx}a_1/F)$ against dimensionless vertical depth for different piezoelectric materials $(PZT-4, (Ba_{0.917}Ca_{0.083})TiO_3)$ and a non-piezoelectric transversely isotropic material (Cadmium)

through Fig. 7(b) and it is evident that frictional coefficient has a favourable effect on induced horizontal electrical displacement. It is to be noted that induced compressive stress, tensile stress and vertical electrical displacement due to a moving load remain unaffected from the friction offered by the upper surface of considered FGPM substrate.

Figs. 8(a) to 10(a) reflect the effect of piezoelectricity on induced compressive stress, shear stress, tensile stress, horizontal electrical displacement and vertical electrical displacement with the variation of vertical depth. The elastic, piezoelectric and dielectric properties of different piezoelectric materials viz. $PZT-4$, $(Ba_{0.917}Ca_{0.083})TiO_3$ and elastic properties of non-piezoelectric material viz. Cadmium are used for this purpose. It is noticed from table (Table 1) that $PZT-4$ is more piezoelectric than $(Ba_{0.917}Ca_{0.083})TiO_3$ while dielectricity of $PZT-4$ is less than $(Ba_{0.917}Ca_{0.083})TiO_3$. In Figs. 8(a) to 8(c), curve 1 corresponds to the situation that irregular functionally graded substrate is without piezoelectricity whereas rest of the curves correspond to the irregular FGPM substrate. Fig. 8(a) reveals the effect of piezoelectricity and dielectricity on induced compressive stress. It has been examined from this figure that the induced compressive stress has minimum value for non-piezoelectric substrate. In case of piezoelectric substrate, as piezoelectricity of the material decreases i.e. dielectricity of the material increases, the induced compressive stress also increases. The effects of piezoelectricity and dielectricity on induced shear stress have been shown by Fig. 8(b). From this figure, it has been found that the substrate with higher extent of piezoelectricity experiences less induced shear stress due to a moving load i.e. dielectricity of the substrate increases the induced shear stress. On the other hand,

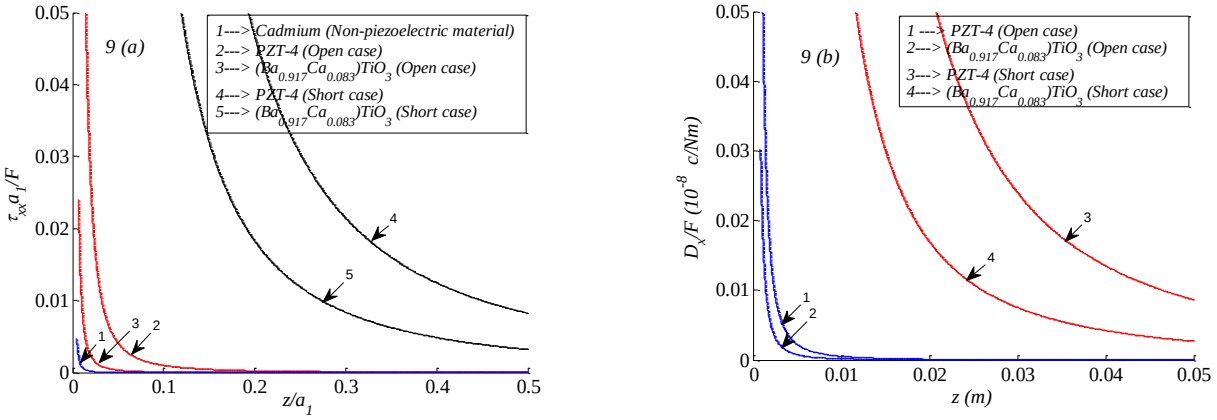

Fig. 9 Variation of (a) dimensionless induced tensile stress $(\tau_{xx}a_1/F)$ against dimensionless vertical depth (z/a_1) (b) induced horizontal electrical displacement (D_x/F) against vertical depth (z) for piezoelectric materials $(PZT-4, (Ba_{0.917}Ca_{0.083})TiO_3)$ and a non-piezoelectric transversely isotropic material (Cadmium)

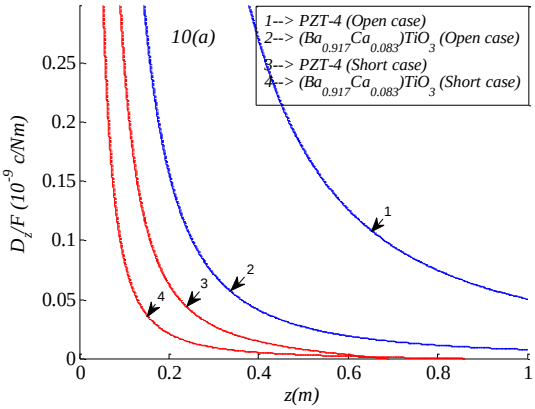

Fig. 10 (a) Variation of induced vertical electrical displacement (D_z/F) against vertical depth (z) for different piezoelectric materials $(PZT-4, (Ba_{0.917}Ca_{0.083})TiO_3)$

induced shear stress is found to be maximum for the case of non-piezoelectric substrate. Figs. 9(a) and 9(b) reflect the effect of piezoelectricity and dielectricity on induced tensile stress and horizontal electrical displacement respectively. It has been examined from these figures that as piezoelectricity of the piezoelectric substrate increases, the induced tensile stress and horizontal electrical displacement also increase while dielectricity of the piezoelectric substrate resists the induced tensile stress and horizontal electrical displacement. It has also been observed from Fig. 9(a) that in case of non-piezoelectric substrate, the minimum values of induced tensile stress are examined as compared to its value in piezoelectric substrate. The effect of piezoelectricity on induced vertical electrical displacement has been delineated by Fig. 10(a). It has been analysed from this figure that piezoelectricity favours and dielectricity opposes the induced vertical electrical displacement due to a moving load on an irregular FGPM substrate.

Through the comparative study of Figs. 2(a) to 10(a), it has been examined that the induced compressive stress and vertical electrical displacement for electrically open condition are more than their values in case of electrically short condition. On the other hand, the induced shear stress, tensile stress and horizontal electrical displacement for electrically short condition are found to be higher as compared to their values in electrically open condition. In addition to this, the comparative analysis suggests that presence of piezoelectricity in irregular functionally graded substrate favours induced tensile stress, horizontal electrical displacement and vertical electrical displacement while it disfavours induced compressive stress and induced shear stress.

5. Conclusions

In present analysis, the maximum incremental compressive stress, shear stress, tensile stress, vertical electrical displacement and horizontal electrical displacement induced due to dynamic load moving with uniform velocity on an irregular transversely isotropic FGPM substrate have been investigated. The influences of various affecting parameters viz. maximum depth of irregularity, irregularity factor, parameter of functionally gradedness, piezoelectricity and dielectricity on induced stresses and electrical displacements have been computed numerically and adduced graphically. The effect of frictional coefficient on induced shear stress and horizontal electrical displacement is also examined. Moreover, the induced stresses and induced electrical displacements due to a moving load have been compared for both electrically open and short conditions and also for presence and absence of piezoelectricity in irregular functionally graded substrate. The following points can be emphasized as the outcomes of the present analysis

1. The closed form expressions of maximum incremental compressive stress, shear stress, tensile stress, horizontal electrical displacement and vertical electrical displacement induced due to a load moving on an irregular transversely isotropic functionally graded piezoelectric substrate have been obtained for both electrically open and short conditions.
2. The induced incremental stresses and induced electrical displacements increase gradually as the maximum depth of irregularity increases for both electrically open and short conditions.
3. The rectangular shaped irregularity has more favourable effect than parabolic shaped irregularity of same depth and span on the induced incremental stresses and electrical displacements while the minimum values of the induced incremental stresses and electrical displacements are found when the FGPM substrate is free from surface irregularity.
4. The functional gradient property discourages induced compressive stress, shear stress, horizontal electrical displacement and vertical electrical displacement for both electrically open and short conditions. On the contrary, it encourages induced tensile stress for both the electrical (open and short) cases.
5. The frictional due to rough upper surface of substrate favours the induced shear stress and induced horizontal electrical displacement for both electrically open and short conditions whereas induced compressive stress, tensile stress and vertical electrical displacement are unaffected from the friction offered by the upper surface of considered FGPM substrate in both the electrical (open and short) cases.
6. The presence of piezoelectricity in irregular functionally graded substrate favours induced tensile stress, horizontal electrical displacement and vertical electrical displacement while it disfavours induced compressive stress and induced shear stress.
7. As the functionally graded piezoelectric substrate becomes more piezoelectric, the induced compressive stress and induced shear stress decreases whereas the induced tensile stress, horizontal electrical displacement and vertical electrical displacement increase.
8. The induced compressive stress and vertical electrical displacement for electrically open condition are more than their values in case of electrically short condition. On the other hand, the induced shear stress, tensile stress and horizontal electrical displacement for electrically short condition are found to be higher as compared to their values in electrically open condition.

The outcomes of the present study may find its possible application in the field of piezo technology for example in road construction where vibrations generated by moving load can be converted into electrical energy and thus harvesting of mechanical waste energy can be done.

Acknowledgments

Authors convey their sincere thanks to Department of Science and Technology, Science & Engineering Research Board (DST-SERB) for their financial support to carry out this research work through Project no. EMR/2016/003985/MS entitled "Mathematical Study on Wave Propagation Aspects in Piezoelectric Composite Structures with Complexities ".

References

Achenbach, J.D., Keshava, S.P. and Herrmann, G, (1967), "Moving load on a plate resting on an elastic half space", *J. Appl. Mech*., **34**(4), 910-914.

Beeby, S.P., Tudor, M.J. and White, N.M. (2006), "Energy harvesting vibration sources for microsystems applications", *Meas. Sci. Technol.*, **17** (12), 175-195.

Chatterjee, M. and Chattopadhyay, A. (2017), "Effect of moving load due to irregularity in ice sheet floating on water", *Acta Mechanica*, 1-17. doi: 10.1007/s00707-016-1786-z.

Chattopadhyay, A., Gupta, S., Sharma, V. K. and Kumari, P. (2011), "Stresses produced on a rough irregular half-space by a moving load", *Acta Mechanica*, **221**(3), 271-280. doi: 10.1007/s00707-011-0507-x.

Chonan, S. (1976), "Moving load on a pre-stressed plate resting on a fluid half-space", *Arch. Appl. Mech*., **45**(3), 171-178. doi: 10.1007/BF00539779.

Cole, J. and Huth, J. (1958), "Stresses produced in a half plane by moving loads", *J. Appl. Mech.*, **25**, 433-436.

De Barros, F.C.P. and Luco J.E. (1994), "Response of a layered viscoelastic half-space to moving point load", *Wave Motion*, **19**(2), 189-210.

Dieterman, H.A. and Metrikine, V. (1997), "Steady-state displacements of a beam on an elastic half-space due to a uniformly moving constant load", *Eur. J. Mech.- A/Solid*s, **16**(2), 295-306.

Du, J., Jin, X., Wang, J. and Xian, K. (2007), "Love wave propagation in functionally graded piezoelectric material layer", *Ultrasonics*, **46**(1), 13-22.

Fryba, L. (1999), *Vibration of solids and structures under moving loads*, (Vol. 1), Springer Science & Business Media.

Haojiang, D. (1996), "General solutions for coupled equations for piezoelectric media", *Int. J. Solids Struct*., **33**(16), 2283-2298.

Hearle, A.D. and Johnson, K.L. (1985), "Mode II stress intensity

factors for a crack parallel to the surface of an elastic half-space subjected to a moving point load", *J. Mech. Phys. Solids*, **33**(1), 61-81.

Kong, L.B., Li, T., Hng, H.H., Boey, F., Zhang, T. and Li, S. (2014), Waste mechanical energy harvesting (I): piezoelectric effect, *Waste Energy Harvesting* (pp.19-128), Springer Berlin Heidelberg.

Li, X.Y., Wang, Z.K. and Huang, S.H. (2004), "Love waves in functionally graded piezoelectric materials", *Int. J. Solids Struct*., **41**(26), 7309-7328.

Meissner, R. (2002), *The little book of planet Earth*. New York: Springer-Verlag.

Mukherjee, S. (1969), "Stresses produced by a load moving over the rough boundary of a semi-infinite transversely isotropic solid", *Pure Appl. Geophys.*, **72**(1), 45-50. doi:10.1007/BF00875691.

Mukhopadhyay, A. (1965), "Stresses produced by a normal load moving over a transversely isotropic layer of ice lying on a rigid foundation", *Pure Appl. Geophys.*, **60**(1), 29-41. doi:10.1007/BF00874804.

Ogawa, T. and Utada, H. (2000), "Coseismic piezoelectric effects due to a dislocation: 1. An analytic far and early-time field solution in a homogeneous whole space", *Phys. Earth Planet. In*., **121**(3), 273-288.

Olsson, M. (1991), "On the fundamental moving load problem", *J. Sound Vib*., **145(**2), 299-307.

Payton, R.C. (2012), *Elastic wave propagation in transversely isotropic media*. (Vol. 4), Springer Science & Business Media.

Piliposian, G.T. and Danoyan, Z.N. (2009), "Surface electro-elastic Love waves in a layered structure with a piezoelectric substrate and two isotropic layers", *Int. J. Solids Struct*., **46**(6), 1345-1353.

Qian, Z., Jin, F., Wang, Z. and Kishimoto, K. (2007), "Transverse surface waves on a piezoelectric material carrying a functionally graded layer of finite thickness", *Int. J. Eng. Science*, **45**(2), 455-466.

Sackman, J.L. (1961), "Uniformly moving load on a layered half plane", *J. Eng. Mech. Div*., **87**(4), 75-90.

Sheng, X., Jones, C.J.C. and Petyt, M. (1999), "Ground vibration generated by a load moving along a railway track", *J. Sound Vib.*, **228** (1), 129-156.

Singh, A. K., Kumar, S. and Chattopadhyay, A. (2014), "Effect of irregularity and heterogeneity on the stresses produced due to a normal moving load on a rough monoclinic half-space". *Meccanica*, **49**(12), 2861-2878.

Singh, A.K., Kumar, S. and Chattopadhyay, A. (2015), "Love-typewave propagation in a piezoelectric structure with irregularity", *Int. J. Eng. Sci*., **89**, 35-60.

Sridhar, S., Giannakopoulos, A.E., Suresh, S. and Ramamurty, U. (1999), "Electrical response during indentation of piezoelectric materials: A new method for material characterization", *J. Appl. Phys*., **85**(1), 380-387.

Tondreau, G., Raman, S. and Deraemaeker, A. (2014), "Point load actuation on plate structures based on triangular piezoelectric patches", *Smart Struct. Syst*., **13**(4), 547-565.

Ungar, A. (1976), "Wave generation in an elastic half-space by a normal point load moving uniformly over the free surface", *Int. J. Eng. Sci*., **14**, 935-945.

Wu, C.P. and Ding, S. (2015), "Coupled electro-elastic analysis of functionally graded piezoelectric material plates", *Smart Struct. Syst.*, **16**(5), 781-806.

Appendix A

$$a=(c_{44}^0q^2+\rho_0V^2-c_{11}^0), b=(c_{44}^0+c_{13}^0)q,$$
$$c=(e_{31}^0+c_{15}^0)q,\ d=\left(c_{33}^0q^2+\rho_0V^2-c_{44}^0\right),\ e=e_{33}^0q^2-e_{15}^0$$
$$\mathrm{A}'=c_{33}^0c_{44}^0\varepsilon_{33}^0+e_{33}^0e_{33}^0c_{44}^0$$
$$B'=\rho_0V^2c_{44}^0\varepsilon_{33}^0-\varepsilon_{33}^0c_{11}^0c_{33}^0+\rho_0V^2c_{33}^0\varepsilon_{33}^0-e_{33}^0c_{11}^0e_{33}^0$$
$$+\rho_0V^2e_{33}^0+2c_{13}^0c_{44}^0e_{33}^0+c_{13}^0c_{13}^0\varepsilon_{33}^0+e_{31}^0c_{44}^0e_{33}^0+c_{33}^0c_{13}^0e_{31}^0$$
$$+e_{15}^0c_{13}^0e_{33}^0$$
$$C'=-\rho_0V^2c_{11}^0\varepsilon_{33}^0-\rho_0V^2c_{44}^0\varepsilon_{33}^0+e_{33}^0c_{11}^0e_{15}^0+{\rho_0}^2V^4\varepsilon_{33}^0+$$
$$c_{11}^0c_{44}^0\varepsilon_{33}^0-\rho_0V^2e_{15}^0e_{33}^0$$
$$\xi_1=c_{13}^0+m_1q_1(c_{33}^0+\gamma e_{33}^0)\ ,\ \xi_2=c_{13}^0+m_2q_2(c_{33}^0+\gamma e_{33}^0),$$
$$\xi_3=c_{44}^0(m_1-q_1)+\gamma m_1e_{15}^0, \xi_4=c_{44}^0(m_2-q_2)+\gamma m_2e_{15}^0,$$
$$\xi_5=-e_{31}^0+m_1q_1(-e_{33}^0+\gamma\varepsilon_{33}^0),\ \xi_6=-e_{31}^0+m_2q_2(-e_{33}^0+\gamma\varepsilon_{33}^0),$$
$$\xi_7=\xi_2\xi_3-\xi_1\xi_4, \xi_8=c_{11}^0+m_1c_{13}^0q_1+\gamma m_1e_{31}^0q_1,$$
$$\xi_9=c_{11}^0+m_2c_{13}^0q_2+\gamma m_2e_{31}^0q_2,\ \xi_{10}=-e_{15}^0q_1+m_1e_{15}^0-\gamma m_1\varepsilon_{11}^0,$$
$$\xi_{11}=-e_{15}^0q_2+m_2e_{15}^0-\gamma m_2\varepsilon_{11}^0$$
$$s_1=q_1^2z^2+(x-Vt)^2,\ s_2=q_2^2z^2+(x-Vt)^2$$
$$\xi_1'=c_{13}^0+m_1q_1c_{33}^0\ ,\ \xi_2'=c_{13}^0+m_2q_2c_{33}^0,\ \xi_3'=c_{44}^0(m_1-q_1),$$
$$\xi_4'=c_{44}^0(m_2-q_2),\ \xi_5'=-c_{31}^0-m_1q_1e_{33}^0,$$
$$\xi_6'=-c_{31}^0-m_2q_2e_{33}^0,\ \xi_7'=\xi_2'\xi_3'-\xi_1'\xi_4'\ ,\ \xi_8'=c_{11}^0+m_1c_{13}^0q_1',$$
$$\xi_9'=c_{11}^0+m_2c_{13}^0q_2',\ \ \xi_{10}'=-e_{15}^0q_1+m_1e_{15}^0,$$
$$\xi_{11}'=-e_{15}^0q_2+m_2e_{15}^0$$

Appendix B

$$A''=\mu(\lambda+2\mu),\ C''=-\rho_0V^2(\lambda+2\mu)-\mu\rho_0V^2-\rho_0^2V^4+\mu(\lambda+2\mu),$$
$$B''=\mu\rho_0V^2-(\lambda+2\mu)^2+\rho_0V^2(\lambda+2\mu)+2\lambda\mu+\lambda(\lambda+2\mu),$$
$$q_i'^2=-\frac{B'''\pm\sqrt{B'''^2-4A'''C'''}}{2B'''}(i=1,2),\ \ a'=\mu q'^2+\rho_0V^2-(\lambda+2\mu),$$
$$b'=(\lambda+\mu)q',\ d'=(\lambda+2\mu)q''^2+\rho_0V^2-\mu,\ m=\frac{a'}{b'}=-\frac{c'}{d'},$$
$$\xi_1''=\lambda+m_1'q_1'(\lambda+2\mu),\ \xi_2''=\lambda+m_2'q_2'(\lambda+2\mu),\ \xi_3''=\nu(m_1'-q_1'),$$
$$\xi_4''=\nu(m_2'-q_2'),\ \xi_5''=0,\ \xi_6''=0,\ \xi_7''=\xi_2''\xi_3''-\xi_1''\xi_4'',$$
$$\xi_8''=(\lambda+2\mu)+m_1'q_1'\lambda,\ \xi_9''=(\lambda+2\mu)+m_2'q_2'\lambda,\ \xi_{10}''=0,\ \xi_{11}''=0$$